Materialwiss. Werkstofftech. **2022**, *53*, 440–448 doi.org/10.1002/mawe.202100347

A small-scale creep test for calibrating an efficient lifetime model for high pressure turbine blades

Ein miniaturisierter Kriechversuch zur Kalibrierung eines effizienten Lebensdauermodells für Hochdruckturbinenschaufeln

C. Dresbach[1], J. Wischek[2], M. Bartsch[2], T. Prien[3]

Jet engines of airplanes are designed such that in some components damage occurs and accumulates in service without being critical up to a certain level of damage. Since maintenance, repair, and component exchange are very cost-intensive, it is necessary to predict efficiently the component lifetime with high accuracy. A former developed lifetime model, based on interpolated results of aerodynamic and structural mechanics simulations, uses material parameters estimated from literature values of standard creep experiments. For improved accuracy, an experimental procedure is developed for the characterization of the short-time creep behavior, which is relevant for the operation of turbine blades of jet engines. To consider microstructural influences resulting from the manufacturing of thin-walled single crystal turbine blades, small-scale specimens from used turbine blades are extracted and tested in short- and medium-time creep experiments. Based on experimental results and literature values, a creep model, which describes the fracture behavior for a wide range of creep loads, is calibrated and is now used for the lifetime prediction of turbine blades under real loading conditions.

Keywords: Nickel-based superalloy **/** lifetime prediction **/** creep **/** gas turbine blade **/** mechanical testing

Flugzeugtriebwerke sind so ausgelegt, dass in einigen Komponenten während des Betriebs Schädigungen auftreten und akkumulieren können, ohne dass diese kritisch werden. Wegen der hohen Kosten von Wartung, Reparatur und Austausch ist es notwendig, die Lebensdauer der Komponenten möglichst effizient und genau vorherzusagen. Ein vorab entwickeltes Lebensdauermodell, welches auf interpolierten Ergebnissen von aerodynamischen und strukturmechanischen Simulationen basiert, nutzt in der Literatur verfügbare Daten aus Standard-Kriechversuchen. Um die Genauigkeit der Lebensdauervorhersage zu verbessern, wird eine Versuchstechnik zur experimentellen Charakterisierung des betriebsrelevanten Kurzzeit-Kriechverhaltens entwickelt. Mikrostrukturelle Einflüsse aus der Herstellung der dünnwandigen einkristallinen Turbinenschaufeln werden berücksichtigt, indem die Proben für die Kriechversuche aus gebrauchten Turbinenschaufeln extrahiert werden. Mit den Daten von Kriechversuchen mit kurzen bzw. mittleren Standzeiten wird nun das Lebensdauermodell kalibriert, so dass für einen weiten Bereich von Kriechlasten das Bruchverhalten von Turbinenschaufeln unter Betriebsbedingungen erfasst wird.

[1] University of Applied Sciences Bonn-Rhein-Sieg, Rheinbach, Germany
[2] German Aerospace Center, Institute of Materials Research, Cologne, Germany
[3] Lufthansa Technik AG, Hamburg, Germany

Corresponding author: C. Dresbach, University of Applied Sciences Bonn-Rhein-Sieg, Von-Liebig-Straße 20, 53359, Rheinbach, Germany,
E-Mail: christian.dresbach@h-brs.de

Schlüsselwörter: Nickelbasis-Superlegierung / Lebensdauervorhersage / Kriechen / Gasturbinenschaufel / Mechanische Prüfung

1 Introduction

The market of maintenance, repair and operation providers is highly competitive and cost driven. Many contracts with customer airlines apply for a duration of multiple years with several shop visits per engine. Often the contracts contain populations of different thrust settings or even sub-fleets with the same engine type but different operations. As customers usually want one offer for all engines, the maintenance provider has to look very carefully into the differences in engine operation, putting pressure on the scrap rate estimation and the work scope strategy as the main cost drivers. Often the risk for unforeseen costs and premature wear lies at the maintenance provider. Therefore, the lifetime estimation of critical and cost intensive engine parts like the high-pressure turbine blades is very important. This becomes even more important when dealing with first time customers, where no or very little historic machine shop data is available or when customers operate under extreme environmental conditions. For many years, the risk-management was very difficult for these special customer groups and made it challenging to create a contract, which was profitable enough for the maintenance provider but yet reasonable for the customer. To change that, Lufthansa Technik developed a lifetime simulation tool for critical engine parts. For a high-quality lifetime estimation accurate physical models are a must-have. In this paper, the calibration of an efficient lifetime model using realistic experimental creep test data is outlined. The testing technique, developed for achieving realistic test data on especially designed miniature specimens, is described, and the results are discussed with respect to an improvement of lifetime prediction accuracy and extension of the model validity due to the now available experimental data.

2 Efficient lifetime prediction approach

The former developed efficient lifetime prediction approach consists of two steps: a high-fidelity design of experiments study and a specific flight history post processor analysis [1], *Figure 1*.

In the first step, a design of experiments study is used for calculating the stress and temperature distributions of three engine components (high pressure turbine blade and vane, low pressure turbine blade) in the relevant parameter range of engine conditions. For this, the correlations between engine parameters were analyzed based on historic data of a whole engine fleet, and a design of experiments scheme with 48 support points was defined. For these 48 engine conditions, the temperature and pressure distributions were calculated with computational fluid dynamic analyses of the whole turbine [1]. With subsequent finite element analyses, the local stress and temperature fields of the above-mentioned engine components were calculated and stored in a large database.

In the second step, an arbitrary engine flight history can by analyzed by interpolating the local stress and temperature distributions in the component of interest based on the design of experiments database and applying a lifetime consumption model on the interpolated stress and temperature fields for each flight. By doing this, it is possible to calculate a whole component life in an acceptable time, e. g. the calculation of the lifetime consumption of a high pressure turbine blade with 2700 take-offs takes about 3 hours of calculations with the postprocessor. In the former investigation, several lifetime consumption approaches were tested [1]. A very promising approach is a modified creep model based on the Larson-Miller relation:

$$D_{\text{creep}} = \frac{t}{t_{\text{r}}(\sigma)} = \left(\exp 10\left(\frac{1000\ L(\sigma)}{T} - 20\right)\right)^{-1} t \tag{1}$$

For describing the short- and longtime behavior, the dependence of the Larson-Miller parameter L is described by an inverted Boltzmann function:

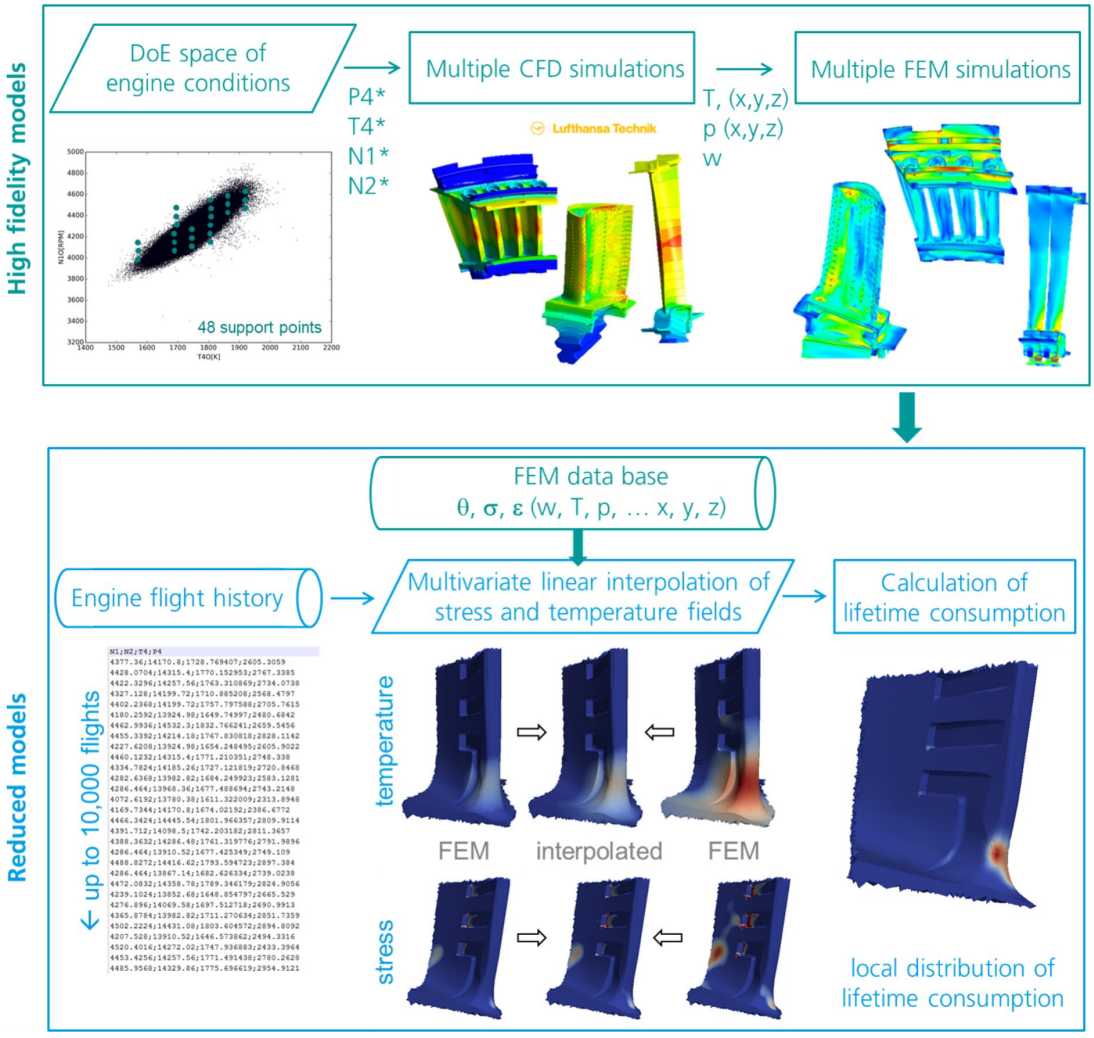

Figure 1. Schematic process of lifetime post processor in accordance with [1].

Bild 1. Schematische Darstellung des Lebensdauer-Postprozessors in Anlehnung an [1].

$$L(\sigma) = \ln\left(\frac{P_0 - P_1}{\sigma_{\mathrm{eqv}} - P_1} - 1\right) P_3 + P_2 \qquad (2)$$

The parameters P_0, P_1, P_2, P_3 were determined by fitting estimated Larson Miller data based on literature values. The validation and the calibration of this model considering small-scale and short time creep experiments is the main intention of this work.

3 Materials and experimental details

3.1 Sample extraction and specimens for mechanical testing

The samples for specimen manufacturing were directly extracted from cooling channel partition walls of original turbine blades made from the single crystalline nickel base superalloy René N5, *Figure 2*. Within this process, first any ceramic thermal barrier coating was removed by grit blasting to allow further electro discharge machining. Then the cover plate of the blade tips was cut away so that the partition walls between the cooling channels were visible and could be extracted.

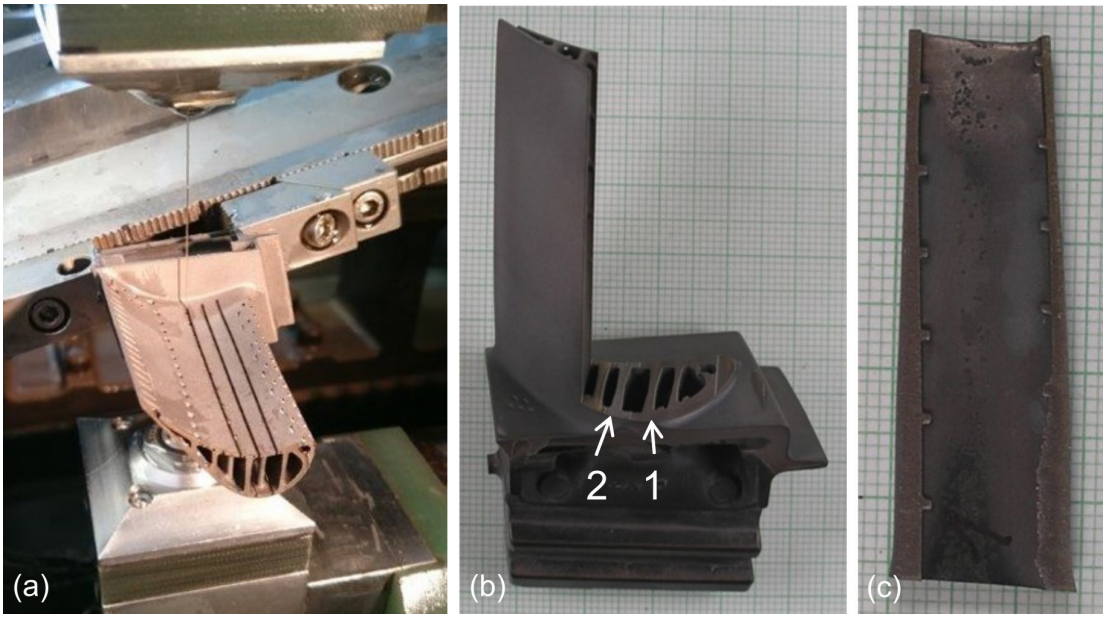

Figure 2. Sample extraction from cooling channel partition walls from a high pressure turbine blade. (a) Cutting by wire electro discharge erosion, (b) location of partition walls suitable for specimen manufacturing, and (c) sample from position 1 in (b).

Bild 2. Probenentnahmen aus den Trennstegen der Kühlkanäle einer Hochdruckturbinenschaufel. (a) Schneiden mittels Drahterosion, (b) Position der für die Probenfertigung geeigneten Trennwände und (c) Probe von Position 1 in (b).

Extracting partition walls for manufacturing test specimens gives the advantage of utilizing already used turbine blades, because the material at the cooling channels is not significantly altered or damaged by the thermal mechanical load history, but displays the typical microstructure of cubic γ' precipitates (nickel aluminide) in a γ-nickel matrix, *Figure 3*.

The thickness and width of the extracted samples vary over the length, and the suitable samples of a turbine blade feature slightly different geometries. To rule out effects of irregular sample geometry, it was decided to manufacture specimens with an hourglass contour, which ensures that nearly the same stress concentrations occur in the gauge length of all specimens. The mechanical load was applied by bolts through circular holes, placed in the specimens far from the gauge length. The evolution of von Mises stresses and plastic strain has been determined for tensile loading by means of finite element calculations, *Figure 4*. Between bolts and holes contact conditions were implemented. The stress concentration is highest at the gauge length, and plastic deformation begins at the gauge length before some local yield occurs at the bolt holes, Figure 4a, b. The difference in stress concen-

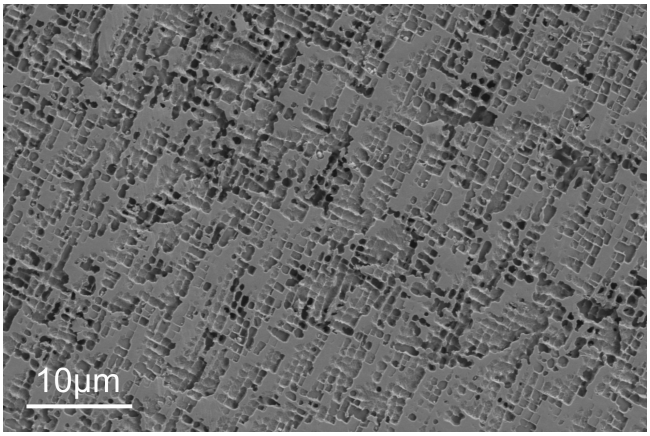

Figure 3. Micrograph by scanning electron microscopy from a polished and etched surface of a cooling channel partition wall extracted from a used turbine blade. Material is René N5, and the micrograph displays the typical microstructure with cubic γ′ precipitates aligned along crystallographic $<100>$ directions.

Bild 3. Mikrostrukturabbildung mittels Rasterelektronenmikroskopie einer polierten und geätzten Oberfläche eines Kühlkanal-Trennsteges, entnommen aus einer gelaufenen Turbinenschaufel. Das Material ist René N5, und das Gefüge zeigt die typische Mikrostruktur mit kubischen γ′ Ausscheidungen, orientiert entlang der kristallografischen $<100>$ Richtungen.

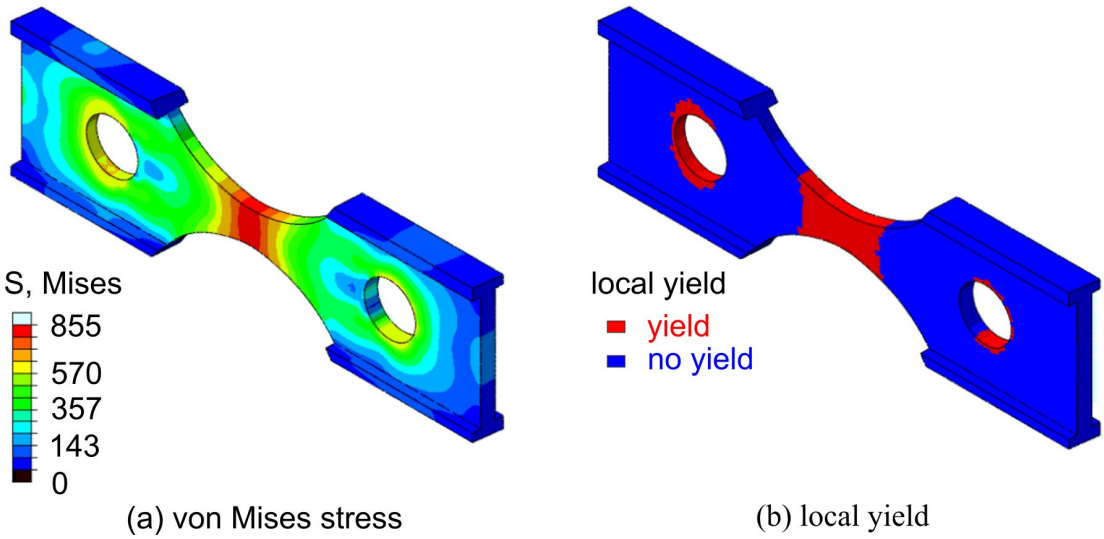

Figure 4. Stress distribution (a) and local yield (b), calculated by finite element simulation for the final specimen geometry under tensile load applied at the bolt holes (von Mises equivalent stresses in MPa).

Bild 4. Spannungsverteilung (a) und lokales Fließen (b), berechnet mittels Finite-Elemente-Simulation der finalen Probengeometrie unter Zugspannung, welche durch die Bolzenlöcher eingeleitet wird (von Mises-Vergleichsspannungen in MPa).

tration and local yield at both bolt holes of a specimen is a consequence of the thickness gradient between the sample ends.

3.2 Mechanical tests

In order to enable mechanical tests under tensile loads at temperatures up to 950 °C, high temperature fixtures for load applications were manufactured. The bolts for load transfer from the grips to the specimens were made from single crystalline nickel base superalloy CMSX-4®, while the grips were made from less expensive polycrystalline nickel base superalloy MAR–M247™.

Tensile tests were performed with a servo-hydraulic testing machine at four different temperatures (ambient, 750 °C, 850 °C, and 950 °C). For specimen heating a 3-zone resistance furnace was used. A comparison of the determined temperature dependence of yield stress and ultimate tensile strength with the literature data, which has been used in the preceding work, shows that the measured ultimate strength values are slightly lower, the yield strength values slightly higher, and the temperatures of the anomalous strength maximum slightly higher compared to literature data [1], *Figure 5*. The high-temperature tensile strength data

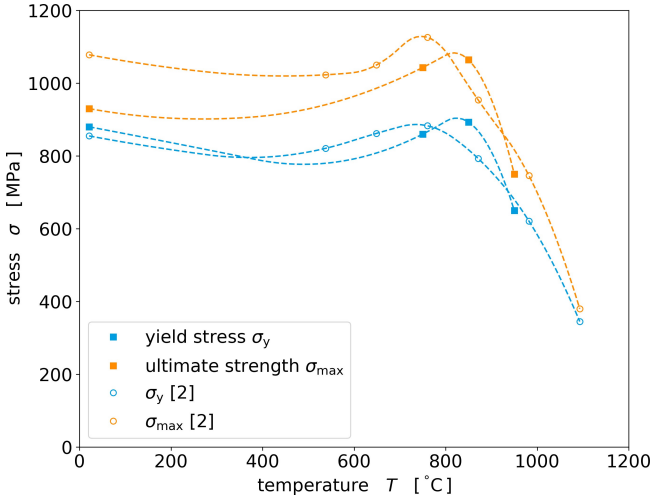

Figure 5. Comparison of temperature dependent yield stress and tensile strength values with literature values from [2].

Bild 5. Vergleich der temperaturabhängigen Dehngrenzen und Zugfestigkeiten mit Literaturwerten aus [2].

have been included in the short-term creep database as described in the following chapter.

The test setup for creep experiments is based on a self-made load frame, *Figure 6*. The load was applied by weights and transferred to the load train of the specimen by means of a lever. For specimen heating a resistance furnace was used. Creep experiments have been performed at 750 °C, 850 °C,

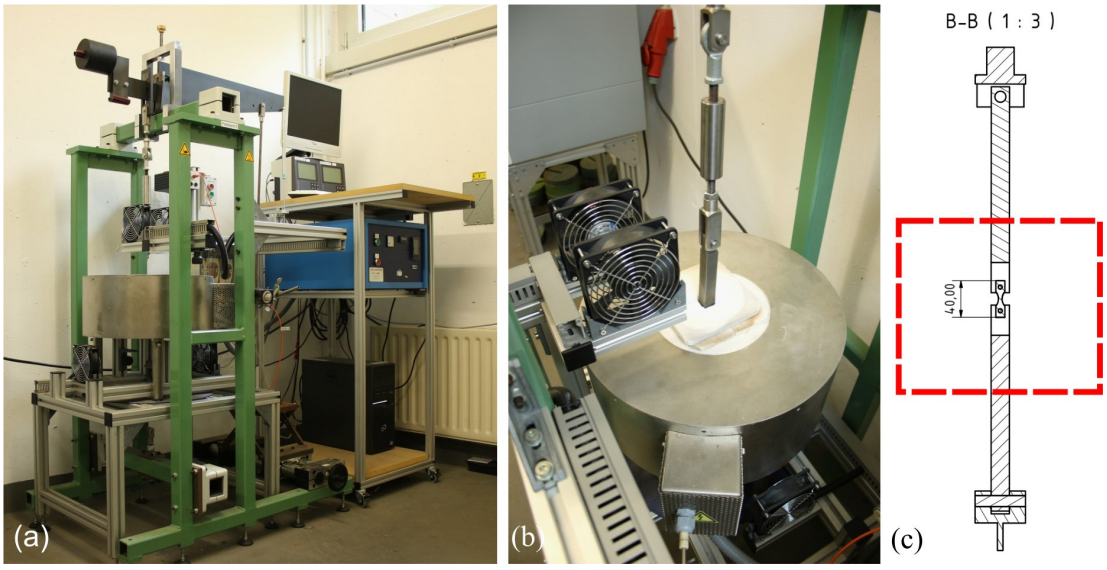

Figure 6. Test setup for small-scale creep testing. (a) Complete system with load frame and a lever for load amplification and (b) resistance furnace to achieve temperatures above 1000 °C; (c) displays the arrangement of specimen, grips, and furnace (indicated by dashed red line).

Bild 6. Testaufbau für Miniaturkriechversuche. (a) Komplettes System mit Lastrahmen und Hebel zur Lastverstärkung; (b) Widerstandsofen für Temperaturen bis 1000 °C; (c) Darstellung des Zusammenbaus von Probe, Halterung und Ofen (gekennzeichnet durch die gestrichelte rote Linie).

and 950 °C. The loading weight was selected with the aim to achieve a pre-defined creep rupture time of 1 h, 10 h, and 100 h, respectively. The achieved creep rupture strength values are slightly higher compared to the predicted data from the original lifetime model, which was based on literature data, *Figure 7*.

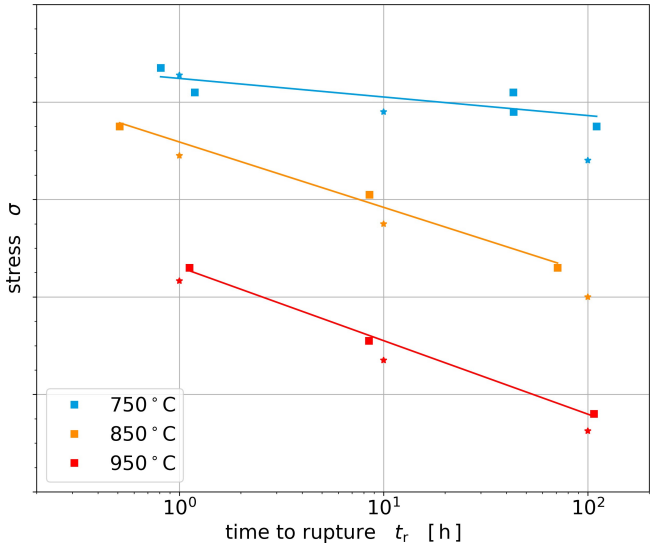

Figure 7. Comparison of the small-scale creep rupture test results (squares) with the prediction of the original lifetime model (stars).

Bild 7. Vergleich der Ergebnisse des miniaturisierten Kriechversuchs (Quadrate) mit der Vorhersage des ursprünglichen Modells (Sterne).

4 Results

4.1 Evaluation of experimental results of tensile tests and creep rupture tests

The experimental results of the tensile tests, the short-time creep tests, and literature values were plotted in a Larson-Miller plot, where the Larson Miller parameter L is calculated from the test temperature T and the time to rupture t_r by equation 3 [2–4]:

$$L = \frac{T\ (20 + \log(t_r))}{1000} \tag{3}$$

The results are consistent for the whole time and temperature regime represented by the Larson-Miller parameter, *Figure 8*. As expected, the Larson-Miller plot shows a horizontal line for small Larson-Miller parameters, representing the short time and low temperature behavior. From that, it is con-

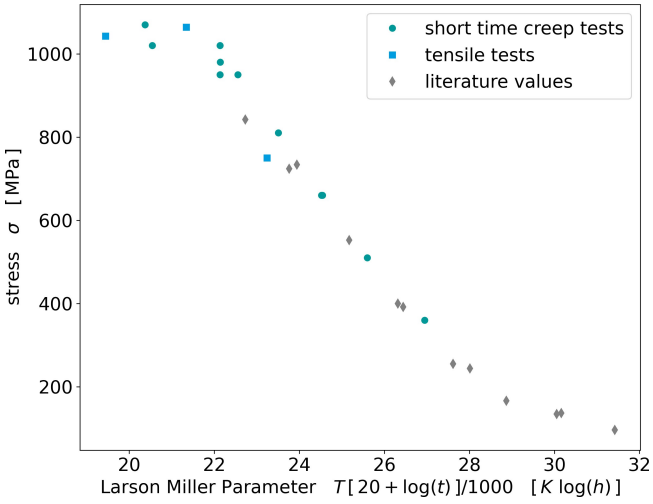

Figure 8. Comparison of the small-scale creep rupture test results with tensile test results and literature values in the Larson-Miller plot.

Bild 8. Vergleich der Ergebnisse des miniaturisierten Kriechversuchs mit den Ergebnissen der Zugversuche und den Literaturwerten in der Larson-Miller-Darstellung.

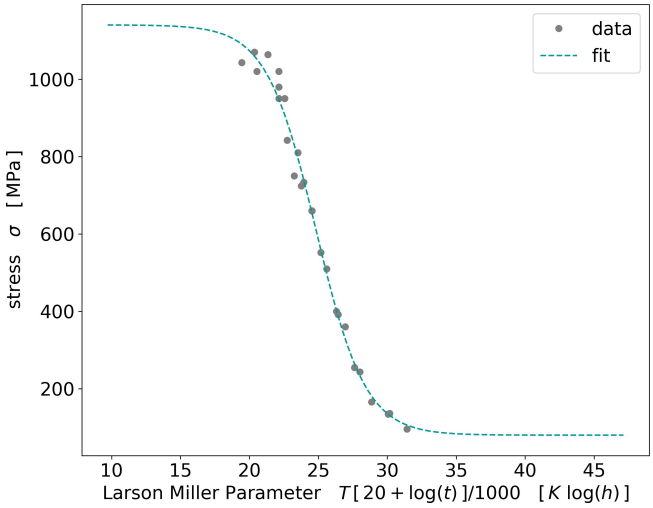

Figure 9. Fit of the combined data from tensile tests, short-time creep test, and literature values in the Larson Miller plot.

Bild 9. Anpassung der kombinierten Daten der Zugversuche, der Kurzzeit-Kriechversuche und der Literaturwerte in der Larson-Miller-Darstellung

cluded, that the short-time creep test results and tensile test results were successfully used to expand the database for lower creep lifetime values.

4.2 Calibration of the creep model

Based on the combined Larson-Miller data of the tensile tests, the short-time creep tests, and the literature values the parameters P_0, P_1, P_2, P_3 according to equation (2) were determined by a data fitting routine with python™. The fit represents well the data in the Larson-Miller plot, and the duration of the creep tests is predicted in good accordance to the experimental creep rupture data, *Figures 9, 10*.

4.3 Application of the creep model

The calibrated creep model described in this paper was transferred into the engine aging prediction environment of Lufthansa Technik. The creep model contributes to a damage factor, which may also include contributions from eventually occurring other damage mechanisms and can be calculated for the high temperature turbine blade of every operator and engine operation. The essence of the simulation is the derivation from the damage result, which represents the damage for only one blade, into a real life scrap-rate, which represents the amount of damaged blades of a whole blade set. This is necessary because of the following fact: During the simulation, the damage prediction for only one single instance of a high pressure turbine blade is calcu-

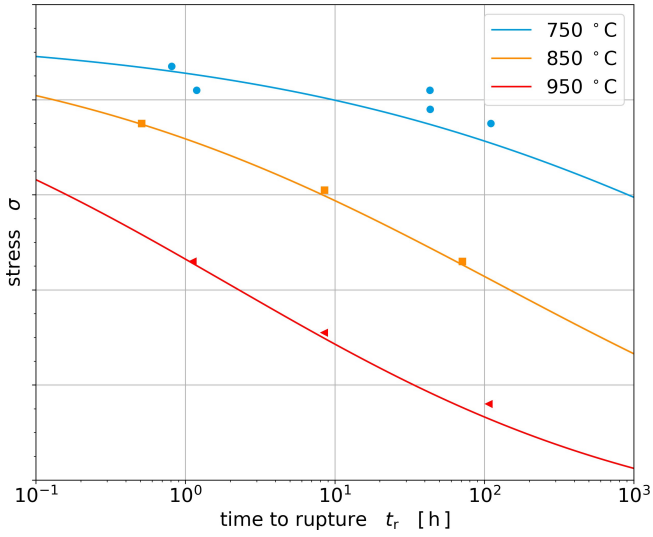

Figure 10. Calculated creep rupture times for constant loads compared with experimental creep rupture test data.

Bild 10. Vergleich der berechneten Kriechbruchzeiten unter konstanter Last mit den experimentell ermittelten Kriechbruchdaten.

lated. However, a high pressure turbine rotor comprises numerous blades, which are not all in the same condition after one run. Very seldom, the whole set of blades is scrap, but typical amount of scrap lies within small and medium to high two-digit percentage values. To get the right amount of scrap for any given airline, the following process has proven successful.

As a baseline, a well-known airline is used, where a large amount of historic data is available, and the scrap-rates are very well known. With this baseline case the damage model and the related scrap-rate estimation has been calibrated. The correlation between amount of calculated damage and real-life scrap-rate is now established and can be used for severity assessments for airlines with unknown scrap-rate, *Figure 11*. The calibrated baseline case enables the maintenance provider to estimate the scrap rates for any given airline during a severity assessment, based on the spatial distribution of accumulated damage, no matter if the operation is moderate or harsh. Sometimes, it can be useful to choose a baseline airline of the same classification (moderate, harsh…) to get the best possible results. Eventually, the results can be translated into an estimated scrap-rate for each one of these airlines, which aids to reduce costs and minimize risks during the offer- and contract-process.

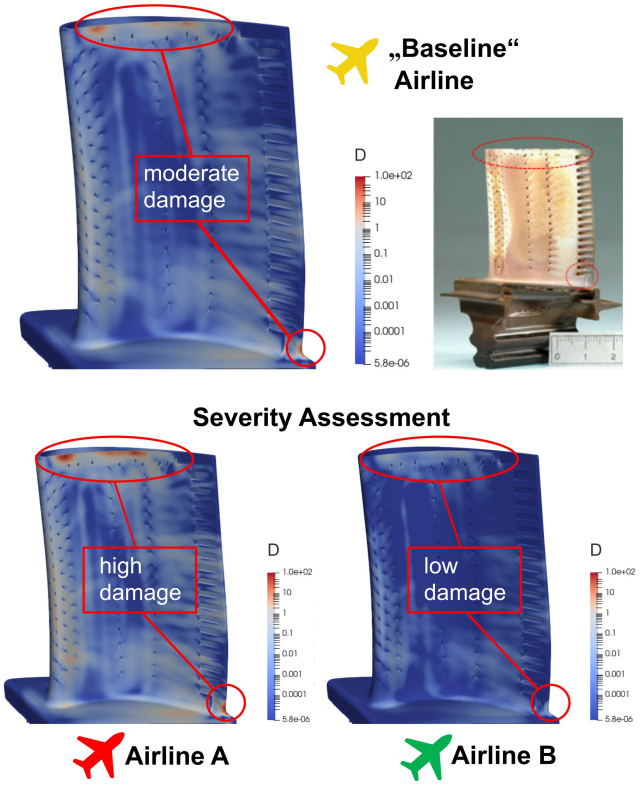

Figure 11. Exemplary illustration of a damage severity assessment process at Lufthansa Technik.

Bild 11. Beispielhafte Darstellung der Schädigungs-Schweregradbeurteilung bei Lufthansa Technik.

5 Summary and discussion

In this work, tensile tests and short-time creep tests with miniaturized creep samples, taken from the cooled regions of discarded high-pressure turbine blades, made of the single crystal alloy René N5, were performed at 750 °C, 850 °C, and 950 °C. With the experimental results, the creep behavior represented in the Larson-Miller plot was extended to the short-time range, which is relevant for the application of turbine components in aero engines. Furthermore, the results confirm that tensile tests can be used for extending the application of the Larson-Miller relation to small Larson-Miller parameters, meaning short time and low temperature behavior. The so verified creep data were used to validate and calibrate the former proposed lifetime consumption model, which is now used in the efficient lifetime prediction approach at Lufthansa Technik.

Acknowledgements

The authors kindly thank B. Fekadu, C. Sick, R. Farahani, R. Kabir, E. Dietrich, and L. Chernova from the German Aerospace Center for supporting and performing the experimental and numerical investigations. Lufthansa Technik funded the experimental study. The lifetime prediction approach was funded by the German Federal Ministry of Economics and Technology embedded in the project “Advanced Prediction Of Severity Effects on Engine Maintenance“ (APOSEM) of the research framework “Luftfahrtforschungsprogramm (LuFo)” under the funding code 20T1308. Open access funding enabled and organized by Projekt DEAL.

6 References

[1] M.J. van Enkhuizen, C. Dresbach, S. Reh, S. Kuntzagk, presented at *ASME Turbo Expo*, June 26–30, **2017**.

[2] Nickel Development Institute, High Temperature High Strength Nickel Base Alloys Supplement, **1995**, 393.

[3] A. Sato, H. Harada, A.-C. Yeh, K. Kawagishi, T. Kobayashi, Y. Koizumi, T. Yokokawa, J.X. Zhang, presented at *Superalloys*, **2008**, pp. 131–138.

[4] R.C. Reed, *The Superalloys, Fundamentals and Applications*, Cambridge University Press, Cambridge, **2006**.

Received in final form: November 22nd 2021

